# Measurement and noise characterization of optically induced index changes using THz interferometry

J. A. Small and R. A. Cheville[a)]
*School of Electrical and Computer Engineering, Oklahoma State University, Stillwater, Oklahoma 74078*

(Received 22 December 2003; accepted 6 April 2004; published online 7 May 2004)

A Michelson interferometer designed for broadband single-cycle THz pulses is used to characterize optically induced index changes in semiconductors which result in submicron changes in optical path length. The interferometric measurements are compared both to standard THz time-domain spectroscopy (THz-TDS) and differential THz-TDS based on modulation of the sample. By analyzing noise contributions in THz spectroscopy systems, it is shown that the destructive interference achieved in THz interferometry reduces both some sources of random errors as well as errors due to system drift. © *2004 American Institute of Physics.* [DOI: 10.1063/1.1758292]

Advances in optical generation and detection of near-single-cycle THz pulses have resulted in ways to measure material properties in the hard-to-access far-infrared spectral region. A variety of characterization techniques based on THz time-domain spectroscopy (THz-TDS) have been developed to measure materials as diverse as semiconductors,[1] flames,[2] and water content.[3] In THz-TDS, a single-cycle electromagnetic pulse with THz bandwidth is used to determine the refractive index and absorption of a sample by comparing the pulse transmitted through the sample to a reference pulse transmitted through dry air. Since THz pulses are near-single cycle with subpicosecond duration, measurement bandwidths can extend from less than 100 GHz to 5 THz.

Because THz-TDS measures transmission changes in a broadband spectrum, it is difficult to accurately characterize materials when the sample is thin, or with low index and/or absorption. When $k(\omega)d \ll 1$—with $k(\omega)$ as the complex frequency dependent wave constant and $d$ as the sample thickness, noise or system drift lead to errors which are greater than the small changes being measured. Recently, several techniques have been developed to characterize thin samples at THz frequencies. One of these is differential time domain spectroscopy (DTDS), which dithers a film on a substrate in and out of the THz beam. By moving the sample so that the boundary of the film moves across the beam, only the modulation induced on the beam by the film is detected. DTDS has been used to determine the refractive index of a 300 nm thick parylene-N film[4] and other thin or low index films.[4–6] By using a double-modulation technique in which both the sample and the THz beam itself are modulated and measured using two lock-in amplifiers,[7] films as thin as 100 nm have been characterized. DTDS substantially increases sensitivity over standard TDS with the primary difficulty ensuring homogeneity of the sample and substrate.

Interferometric techniques have also been used to measure small changes to a THz beam.[8,9] In this case, destructive interference occurs between simultaneously measured sample and reference pulses. By eliminating the background signal, some noise sources and drift are eliminated. In this letter, we demonstrate THz interferometric characterization of optically induced index changes in a high resistivity silicon wafer, permitting direct comparisons between THz interferometry, THz-TDS, and DTDS. Both THz interferometry and DTDS give comparable results. Following previous treatments of noise sources in THz-TDS,[10] improvements in resolution are shown to cause a reduction in emitter noise compared to THz-TDS.

The experimental setup consists of a THz-TDS system[1] configured as a Michelson interferometer,[8] shown in Fig. 1. The THz emitter is a coplanar transmission line fabricated on semi-insulating GaAs and biased at 80 $V_{dc}$, which generates freely propagating pulses of THz electromagnetic radiation.[1] The incident optical excitation beam is modulated at $f_{THz} = 1650$ Hz by a mechanical chopper. The generated THz radiation is collimated by a silicon lens and parabolic mirror. A 1.0 mm thick $n$-type high resistivity ($>10$ kΩ cm) silicon

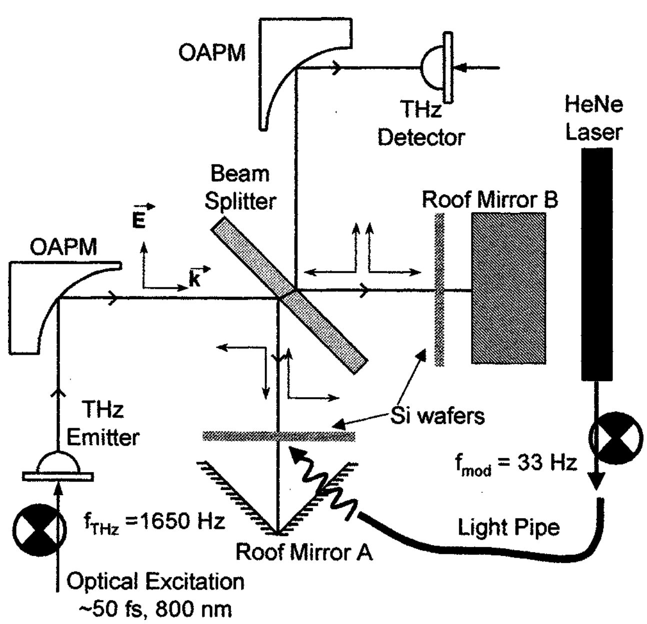


FIG. 1. Experimental setup of THz interferometer. Sub-100 fs pulses at 820 nm are used to generate the THz pulses while optical excitation of the sample is using a HeNe laser at 632 nm.

[a)]Author to whom correspondence should be addressed; electronic mail: kridnix@okstate.edu

 

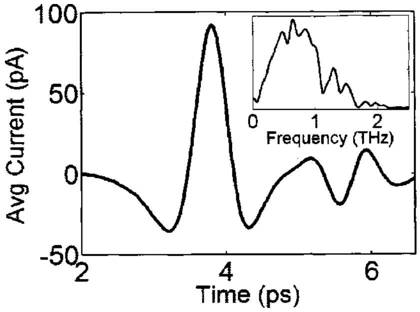


FIG. 2. THz pulse from sample arm (A). The inset shows the spectral amplitude, $S(\omega)$ obtained by a numerical Fourier transform. The reference arm spectrum, $R(\omega)$, is nearly identical. The oscillations after the pulse and valleys in the spectrum are due to atmospheric water vapor.

slab is used as a beam splitter to divide the THz beam into $E_A$ and $E_B$ pulse trains.[8] Front surface aluminum-coated roof reflectors, labeled A and B in Fig. 1, are oriented such that the incident THz beam is P polarized at reflector A and S polarized at reflector B. The P-polarized beam undergoes a frequency independent $\pi$ phase shift due to the rotation of the electric field during reflection. The pulse detected by the THz detector is thus a superposition of the pulse in the reference arm, B, and $\pi$ phase shifted pulse from the arm with the sample, A. The time-resolved electric field of the superposition of reference and sample THz pulses is measured with an optically gated 30 $\mu$m dipole antenna[11] with a silicon lens to collect the incident THz radiation. The current induced in the dipole is measured using a current amplifier and lock in with a 100 ms integration time. The superposition signal has an amplitude of less than 5% of the signal in either arm A or B separately.

The materials to be characterized, in this case 1.00 mm thick, double-side polished, $>10$ k$\Omega$ cm silicon wafers, are inserted in each arm as shown in Fig. 1. The wafer in arm A (sample) is illuminated by a continuous-wave HeNe laser (632.8 nm) incident at the Brewster angle of 76°. The fluence incident on the silicon wafer is controlled using a variable attenuator, measured with a calibrated power meter. The measured THz pulse measured in arm A (arm B blocked) is shown in Fig. 2; the inset shows the measurement bandwidth of 0.3–2.0 THz obtained by a numerical Fourier transform. The spectral valleys are due to absorption by atmospheric water vapor; experiments were performed in ambient air.

For DTDS measurements, the incident HeNe beam is modulated by an optical chopper at $f_{\mathrm{mod}}=33$ Hz, and two lock-in amplifiers are used to enhance signal to noise.[7] The first lock-in amplifier has a reference frequency of $f_{\mathrm{THz}}$, an integration time of 1 ms, and is used to measure the incident THz pulse. The output from the first lock in is sent to a second lock-in amplifier with a reference frequency $f_{\mathrm{mod}}$ and 1 s integration time that are used to detect the optically induced change in transmission of the THz pulse.

To determine the effect of noise and signal drift on sample characterization using THz-TDS and THz interferometry, we follow the treatment of Duvillaret, *et al.*[10] For THz-TDS, the noise contributions are analyzed using the measured sample, $S(\omega)$, and reference, $R(\omega)$, frequency dependent spectral amplitudes. These are obtained from numerical Fourier transforms of the THz pulses transmitted through the sample arm, A, with and without optical illumination. For THz-TDS the complex transmission coefficient is defined as $T(\omega)=S(\omega)/R(\omega)=\rho(\omega)e^{i\varphi(\omega)}$, from which the real part of the complex refractive index, $n(\omega)=n'(\omega)-in''(\omega)$, is extracted from the argument, $\varphi(\omega)$, and the absorption coefficient, $\alpha(\omega)=\omega n''(\omega)/c$, from the modulus, $\rho(\omega)$.

Errors in the measurement of $n(\omega)$ are proportional to the variance of the modulus, $\sigma_\rho^2(\omega)$, which in turn is related to the variance of the reference, $\sigma_R^2(\omega)$, and sample, $\sigma_S^2(\omega)$, data scans:[10]

$$\sigma_\rho^2(\omega)=\frac{\sigma_s^2(\omega)}{|R(\omega)|^2}+\frac{\rho(\omega)}{|R(\omega)|^2}\sigma_R^2(\omega). \tag{1}$$

As in the case here, when $\rho(\omega)$ approaches unity:

$$\sigma_\rho^2(\omega)=\frac{2\sigma_{\mathrm{noise}}^2(\omega)}{|R(\omega)|^2}. \tag{2}$$

Noise contributions on the sample or reference scans arise from three sources:[10]

$$\sigma_{\mathrm{noise}}^2(\omega)=\rho^2(\omega)\sigma_e^2(\omega)+\sigma_{\mathrm{sh}}^2(\omega)+\sigma_d^2(\omega) \tag{3}$$

where for thin sample $\rho(\omega)\cong 1$. These three terms correspond to noise from the THz emitter $\sigma_e^2(\omega)$, shot noise in the THz detector $\sigma_{\mathrm{sh}}^2(\omega)$, and other signal independent noise sources, $\sigma_d^2(\omega)$ such as laser noise, electronic noise, and Johnson noise.[10,12] The shot noise can be written as $\sigma_{\mathrm{sh}}^2(\omega)=2e\Delta fX(\omega)$ with $e$ as the electron charge, $\Delta f$ the measurement bandwidth determined by the lock-in integration time, and $X(\omega)$ either $R(\omega)$ or $S(\omega)$. As shown in Ref. 10, the dominant noise term comes from the THz emitter, $\sigma_e^2(\omega)$, especially in the case of slightly absorbing samples with $\rho(\omega)$ approaching unity, and $S(\omega)\cong R(\omega)$. For THz-TDS, the sample and reference scans are measured independently and the noise on the sample and reference scans are uncorrelated.

For THz interferometry, a more relevant noise figure is given by the variance of the measured interference signal, $D(\omega)=R(\omega)-S(\omega)$. Since in THz interferometry the difference is obtained in a single measurement, the emitter noise is correlated between the sample arm (A) and reference arm (B). The noise on the interferometric signal can thus be written:

$$\sigma_{\mathrm{int}}^2(\omega)=(1-\rho(\omega))^2\sigma_e^2(\omega)+2e\Delta fR(\omega)(1-\rho(\omega))+2\sigma_d^2(\omega). \tag{4}$$

For $k(\omega)d\ll 1$, the modulus of the difference signal, $1-\rho(\omega)$, is proportional to $|\omega dn(\omega)/cR(\omega)|$ in the case of transparent, $n'(\omega)\gg n''(\omega)$, or lossy, $n'(\omega)\ll n''(\omega)$, samples.[8] A comparison of Eq. (3) with Eq. (4) shows that the effects of both the shot noise and emitter noise are substantially reduced in THz interferometry. The previous analysis assumes ideal cancellation of the two arms of the interferometer; in an actual experimental configuration interference of the sample and reference pulses can achieve approximately 95% amplitude cancellation due to lack of rotational symmetry of the THz beam.[8,13]

To demonstrate that THz interferometry can distinguish small changes in a sample, we utilize optical modulation of the refractive index of a high resistivity, $>10$ k$\Omega$ cm silicon

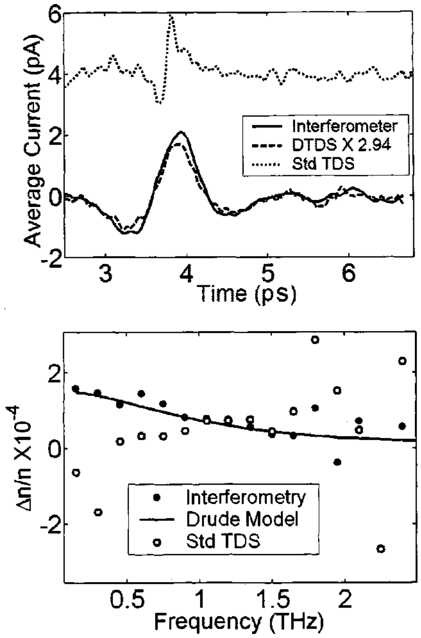


FIG. 3. (a) THz pulses measured using THz interferometer (solid line), DTDS (dashed line), and the difference between two consecutive THz scans taken with and without optical excitation (dotted line). (b) Optically induced change in refractive index determined from THz interferometry (dots), THz-TDS (open circles), and Drude theory (line).

wafer. As shown in Fig. 1, 2 eV photons incident at Brewster's angle create free carriers. The frequency dependent change in refractive index, $\Delta n(\omega)=\sqrt{\varepsilon_r(\omega)}$, is described by the Drude model:[14]

$$\varepsilon_r(\omega)=\varepsilon_\infty-\sum_{j=e,h}\frac{\omega_p^2}{\omega(\omega+i\Gamma_j)} \tag{5}$$

where $\varepsilon_\infty=11.7$ is the relative permittivity of Si, $\omega_p$ is the electron or hole plasma frequency given by $\omega_p^2=Ne^2/\varepsilon_0 m_{e,h}^*$ with free-space permittivity $\varepsilon_0$, carrier density N assumed equal for electrons and holes, and effective masses $m_e^*=0.26$ and $m_h^*=0.37$.[15] $\Gamma_j$ is the carrier damping rate $1/\tau_{e,h}$.[14] For the $>10$ k$\Omega$ cm Si sample, the only appreciable contributions to the free carrier density are those carriers generated by optical modulation. For these measurements, the excitation intensity used, $3.58\times10^{-2}$ mW/cm$^2$, results in a carrier density of $N=6.53\times10^{12}$ cm$^{-3}$. We assume that the carrier density across the sample is uniform since the carrier recombination time of $\tau_r=25$ ms corresponds to a diffusion length greater than 2 mm at low carrier densities.[16]

Figure 3(a) compares the difference between two consecutive THz scans taken with and without optical excitation (dotted line), a single data scan taken using DTDS (dashed line), and a scan on the THz interferometer (solid line) with the constant background signal numerically subtracted.[8] The DTDS scan has been normalized to the throughput of the THz interferometer (34.7%). The ratio between peak signal and background noise of the difference signal is 4.9:1. For the data scan using the THz interferometer, the ratio is 21:1 while that of the DTDS measurement is 22:1.

Figure 3(b) plots the measured optically induced change in refractive index, $\Delta n(\omega)/n(\omega)$, obtained from THz interferogram (points) and that determined by THz-TDS (open circles), both using the Fourier transform of the temporal data of Fig. 3(a) where

$$\Delta(n_r(\omega)-in_i(\omega))=-i\frac{c}{\omega d}\ln\left(\frac{R(\omega)-D(\omega)}{R(\omega)}\right). \tag{6}$$

The index change calculated using Drude theory is shown as a solid line in Fig. 3(b). The measured index changed was determined taking into account the Fresnel transmission coefficients on the input and output faces of the Si wafer, but not the Fabry–Perot term[10] since reflections from the wafer faces were time gated out. Using THz interferometry, index changes of $10^{-4}$ can be measured, which corresponds to a change in the optical path length of 342 nm. The same measurement made using THz-TDS only closely approximates the actual index change over a small frequency range. At 0.7 THz, the peak of the THz amplitude spectrum, 342 nm is an optical path length change of $\lambda/1250$. Extrapolating the results to a unity signal-to-noise ratio, the measurement limit of the system is 32 nm or $\lambda/13\,500$.

We have demonstrated that THz time-domain interferometry can measure photoinduced refractive index change at THz frequencies of $\Delta n/n<10^{-4}$, and demonstrated sensitivity to changes in optical path length comparable to those previously obtained with DTDS.[6] For thin-film measurements, DTDS utilizes spatial dithering of the THz beam across a step boundary of the film while THz interferometry needs an identical reference substrate. Analysis of noise sources of THz-TDS, fully treated in Ref. 10, show that the measurement sensitivity arises from a reduction of both emitter and shot noise.

The authors would like to acknowledge support from the National Science Foundation (ECS-9984896), Army Research Office (DAAD19-99-R-BAA8), and Department of Energy. One of the authors (J.S.) acknowledges support of the NSF IGERT program for support during this work.

[1] D. Grischkowsky, S. Keiding, M. van Exter, and C. Fattinger, J. Opt. Soc. Am. B **7**, 2006 (1990).
[2] R. A. Cheville and D. Grischkowsky, Opt. Lett. **20**, 1646 (1995).
[3] D. M. Mittleman, R. H. Jacobsen, and M. C. Nuss, IEEE J. Sel. Top. Quantum Electron. **2**, 679 (1996).
[4] K.-S. Lee, T.-M. Lu, and X.-C. Zhang, Microelectron. J. **34**, 63 (2003).
[5] Z. P. Jiang, M. Li, and X. C. Zhang, Appl. Phys. Lett. **76**, 3221 (2000).
[6] M. L. Z. Jiang and X.-C. Zhang, J. Appl. Phys. **76**, 3221 (2000).
[7] M. Brucherseifer, P. H. Bolivar, and H. Kurz, Appl. Phys. Lett. **81**, 1791 (2002).
[8] S. Krishnamurthy, M. T. Reiten, S. A. Harmon, and R. A. Cheville, Appl. Phys. Lett. **79**, 875 (2001).
[9] J. L. Johnson, T. D. Dorney, and D. M. Mittleman, Appl. Phys. Lett. **78**, 835 (2001).
[10] L. Duvillaret, F. Garet, and J.-L. Coutaz, J. Opt. Soc. Am. B **17**, 452 (2000).
[11] M. van Exter, C. Fattinger, and D. Grischkowsky, Appl. Phys. Lett. **55**, 337 (1989).
[12] M. van Exter and D. R. Grischkowsky, IEEE Trans. Microwave Theory Tech. **38**, 1684 (1990).
[13] M. T. Reiten, S. A. Harmon, and R. A. Cheville, J. Opt. Soc. Am. B **20**, (2003).
[14] M. van Exter and D. Grischkowsky, Phys. Rev. B **41**, 12140 (1990).
[15] D. Grischowsky and T.-I. Jeon, Phys. Rev. Lett. **78**, 1106 (1996).
[16] S. M. Sze, *Physics of Semiconductor Devices* (Wiley, New York, 1981).